small NANO MICRO

Polymorphism of Phosphine-Protected Gold Nanoclusters: Synthesis and Characterization of a New 22-Gold-Atom Cluster

*Qian-Fan Zhang, Paul G. Williard, and Lai-Sheng Wang**

***A** new Au_{22} nanocluster, protected by bis(2-diphenyl-phosphino)ethyl ether (dppee or $C_{28}H_{28}OP_2$) ligand, has been synthsized and purified with high yield. Electrospray mass spectrometry shows that the new cluster has a formula of $Au_{22}(dppee)_7$, containing 22 gold atoms and seven dppee ligands. The cluster is found to be stable as a solid, but metastable in solution. The new cluster has been characterized by UV-Vis-NIR absorption spectroscopy, collision-induced dissociation, and ^{31}P-NMR. The properties of the new cluster have been compared with the previous $Au_{22}(dppo)_6$ nanocluster (dppo = 1,8-bis(diphenyl-phosphino)octane or $C_{32}H_{36}P_2$), which contains two fused Au_{11} units. All the experimental data indicate that the new $Au_{22}(dppee)_7$ cluster is different from the previously known $Au_{22}(dppo)_6$ cluster and represents a new Au_{22} core, which contains most likely one Au_{11} motif with several $Au_2(dppee)$ or $Au(dppee)$ units. The $Au_{22}(dppee)_7$ cluster provides a new example of the ligand effects on the nuclearity and structural polymorphism of phosphine-protected atom-precise gold nanoclusters.*

1. Introduction

Ligand-protected gold nanoclusters (AuNCs) have attracted tremendous interest recently, due to their potential applications in catalysis, biosensor, imaging, and molecular electronics.[1,2] Unlike conventional gold nanoparticles, AuNCs consist of only a few or tens of gold atoms protected by ligands. They have atomically precise molecular formulas and well-defined coordination geometries. The quantum confinement effects of such small gold cores lead to discrete electronic states, which give rise to unique molecular-like electronic properties for AuNCs. The monodispersity and well-defined geometry make AuNCs ideal models for understanding structure-property relationships.

By controlling the size and shape of the core geometry and the type of ligands, a variety of atomically precise AuNCs may be synthesized with new structures and properties. The type of ligand is especially important, because of the different metal-ligand interactions. To date, AuNCs have been synthesized using thiolates/selenolates,[3–23] alkynyls,[24–26] phosphines,[27–55] or mixed ligands.[28–31] In particular, a wide range of AuNCs with the thiolate/selenolate ligands have been synthesized and structurally characterized with gold cores ranging from Au_{18}[3,4] to Au_{133},[22,23] since the first synthesis and structural determination by X-ray crystallography of the Au_{102} cluster using the *para*-mercaptobenzoic acid ligand.[20] Thiolate-protected AuNCs have all been found to have complicated gold-ligand interfaces, because of the formation of gold-thiolate staples.[20] From the structural point of view, the ligands that protect the core are actually gold-thiolate staples, which should be treated as multidentate ligands. Hence, the true gold cluster cores are in fact smaller than the AuNC formulas indicate. Similar staples have also been found in the alkynyl-protected Au_{19},[24] Au_{23},[25] and Au_{24}.[26] On the other hand, phosphine-protected AuNCs tend to have simpler interfaces with well-defined cores and ligand layers,[27–31] due

Q. F. Zhang, Prof. P. G. Williard, Prof. L. S. Wang
Department of Chemistry
Brown University
Providence, RI 02912, USA
E-mail: lai-sheng_wang@brown.edu

DOI: 10.1002/smll.201600407

to the neutral charge state of phosphines and the weaker gold-phosphine bond. The simpler interface and weaker Au-phosphine bond may allow better control of the core size and potentially allow more convenient access to the gold core in catalytic reactions.

The crystal structures of small phosphine-protected AuNCs (nuclearity ≤ 13) have been well studied.[27] It is interesting to note that many of these AuNCs, such as Au_6,[34–36] Au_7,[37,38] Au_8,[39,40] Au_9,[41,42] Au_{10},[43,44] and Au_{11},[45–47] have at least two different core geometries when different phosphine ligands are used. However, beyond Au_{13}, only four different phosphine-protected AuNCs have been structurally characterized by X-ray crystallography, including Au_{14},[48] Au_{20},[49–51] Au_{22},[52] and Au_{39}.[53] It should be pointed out that two different Au_{20} core structures have been reported using different ligands.[49–51] In addition, two larger AuNCs with phosphine ligands, i.e., Au_{55} and Au_{75},[54,55] have been reported, but they have not been crystallized.

The bare Au_{20} cluster was found in the gas phase to have a tetrahedral pyramidal structure (T_d).[56] All the 20 Au atoms of the Au_{20} pyramid are on the cluster surface, which would make it an ideal model for catalysis. The pyramidal structure has been observed by high-resolution electron microscopy for size-selected Au_{20} deposited on a carbon substrate in vacuum.[57] The Au_{20} pyramid was observed to be present in solution with triphenylphosphine (PPh_3) ligands using a synthetic procedure for gold nanoparticles.[58] The pyramidal structure and the electronic properties of the T_d $Au_{20}(PPh_3)_4$ cluster were shown computationally to be similar to those of the bare Au_{20}.[58] However, in order to obtain large quantities of pure pyramidal Au_{20} samples and investigate its interesting catalytic and optical properties, a high yield synthetic method is needed. One of the strategies that we have been pursuing is to use diphosphine ligands with different chain lengths.[59] Using the 1,8-bis(diphenyl-phosphino) octane (dppo for short), we have synthesized a $Au_{22}(dppo)_6$ cluster with a relatively high yield.[52] Structural determination using single crystal X-ray diffraction revealed that the Au_{22} core in $Au_{22}(dppo)_6$ contained two fused Au_{11} units. Interestingly, there are eight Au atoms at the interface of the two Au_{11} units that were not coordinated by the dppo ligands.

Here we report the synthesis of a new Au_{22} cluster using the bis(2-diphenyl-phosphino)ethyl ether (dppee or $C_{28}H_{28}OP_2$) ligand, which has a slightly shorter chain length than the dppo ligand[52] and can be viewed as replacing four CH_2 groups in dppo by an ether group. The new Au_{22} cluster is found to be coordinated by seven dppee ligands, $Au_{22}(dppee)_7$, and can be obtained with relatively high yield and purity. The yield (~25% based on Au atoms) is higher than the syntheses of most AuNCs,[3–31] which usually have yields ≤ 16%. The $Au_{22}(dppee)_7$ cluster has been characterized by UV-Vis-NIR, collision-induced dissociation (CID), and ^{31}P-NMR and compared with the previous $Au_{22}(dppo)_6$ cluster.[52] It is concluded that the new $Au_{22}(dppee)_7$ nanocluster has a totally different core structure from the previous $Au_{22}(dppo)_6$ cluster. The current work provides another example of controlling high-nuclearity Au core structures by different ligands and the polymorphism of AuNCs by phosphine ligands.

2. Results

2.1. Synthesis of $Au_{22}(dppee)_7$

The details of the synthetic and characterization methods are described in the Experimental Section. The $Au_{22}(dppee)_7$ nanoclusters were synthesized in a single step reaction followed by purification, which was different from most thiolate-protected AuNCs and some small size phosphine-protected AuNCs.[60,61] The latter all have a special long etching process, in order to obtain the most stable products. However, in the current synthesis of the $Au_{22}(dppee)_7$ nanocluster, longer etching time did not result in better yield or purity of the final product.

2.2. Optimization of Synthetic Conditions Using Electrospray Ionization Mass Spectrometry and UV-Vis-NIR Absorption Spectroscopy

We used electrospray ionization mass spectrometry (ESI-MS) to monitor and optimize the synthesis. In preparation of the ESI solution, a small amount of formic acid (0.05%) was added to facilitate ionization and provided the protons for many ESI-MS peaks in the positive ion mode. Consequently, the $Au_{22}(dppee)_7$ nanocluster was observed in the ESI-MS in the form of a $[Au_{22}(dppee)_7H_3]^{3+}$ ion, similar to our previous observation for the $Au_{22}(dppo)_6$ nanocluster, which was observed in the form of $[Au_{22}(dppo)_6H_4]^{2+}$.[52] The relative intensity of the $[Au_{22}(dppee)_7H_3]^{3+}$ ion peak in the ESI-MS did not change dramatically, when the reaction time was increased from 20 hto 120 h, as shown in **Figure 1**a, which also revealed mass peaks related to the starting material and a few byproducts. The similar intensity of the $[Au_{22}(dppee)_7H_3]^{3+}$ peaks after 20 h and 120 h indicated that the $Au_{22}(dppee)_7$ nanocluster is a relatively stable product.

UV-Vis-NIR spectra (**Figure 2**a) also showed no significant changes at the 20 h or 120 h reaction times, consistent with the ESI-MS results. The only differences in the two UV-Vis-NIR spectra were the relative intensities of the absorption peaks at ≈410 and 305 nm, which turned out not to be due the absorptions of pure $Au_{22}(dppee)_7$. Figure 2b displayed the UV-Vis-NIR spectra of pure $Au_{22}(dppee)_7$ dissolved in CH_2Cl_2 after column separation (vide infra). These spectra were taken for freshly separated samples and at different times after the separation, showing that significant changes occurred after 3 d in solution. The $Au_{22}(dppee)_7$ cluster was much more stable as a solid, for which significant changes were only observed after 9 d. The time-dependent UV-Vis-NIR spectra suggested that the formation of the $Au_{22}(dppee)_7$ nanocluster might be kinetically controlled. In order to explore the formation kinetics, we carried out syntheses at different temperatures: –20, 0, 20, and 40 °C. We found the best yield was ≈25% at 20 °C, followed by ≈18% at 0 and 40 °C, then <7% at –20 °C. The slow reaction rate at low temperatures caused a decrease in yield, while at high temperatures the $Au_{22}(dppee)_7$ cluster might be converted to other products to also give a low yield.

small 2016,
DOI: 10.1002/smll.201600407

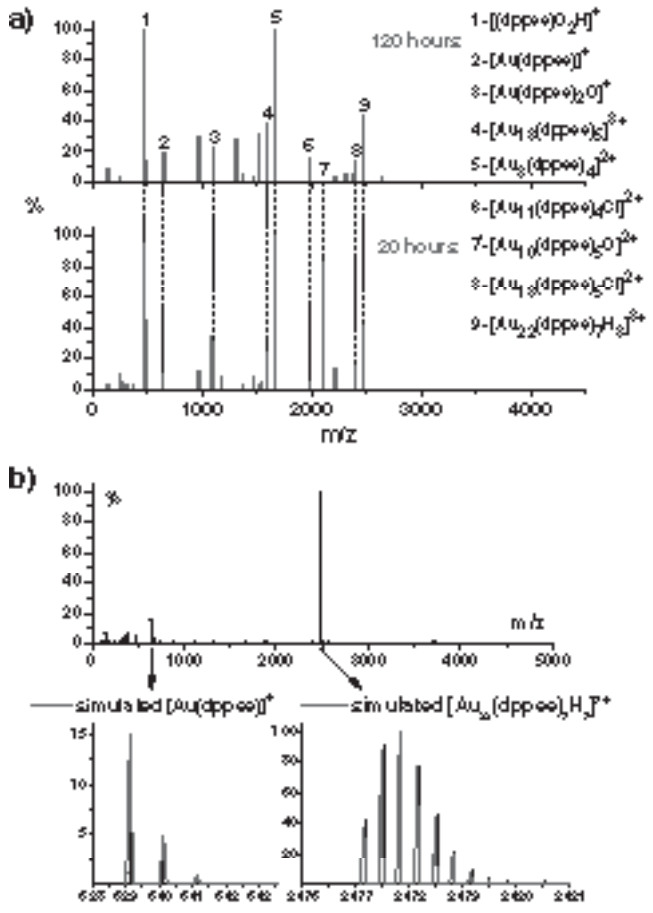

Figure 1. a) Electrospray mass spectra of the crude products during the syntheses of $Au_{22}(dppee)_7$ with different reaction times. b) Electrospray mass spectra of pure $Au_{22}(dppee)_7$ after column separation, as well as the experimental and simulated isotopic distributions of the two major peaks. (Mobile phase of ESI: acetonitrle/water = 50/50, 0.05% formic acid).

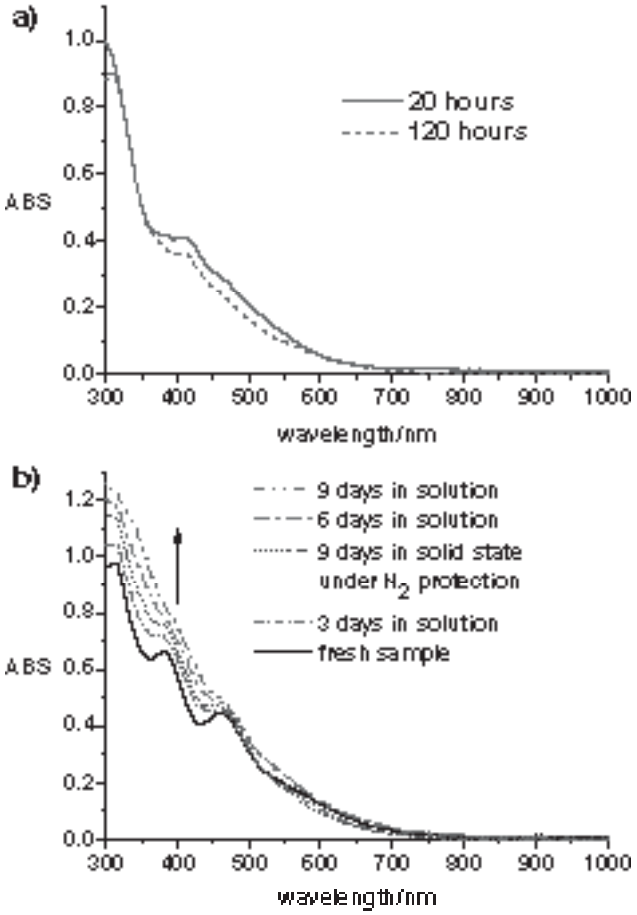

Figure 2. a) UV-Vis-NIR of the crude products during the syntheses of $Au_{22}(dppee)_7$ with different reaction times. b) UV-Vis-NIR spectra of pure $Au_{22}(dppee)_7$ after column separation in CH_2Cl_2 solution and the test of its shelf life. The spectrum of a pure solid sample is also shown for comparison.

2.3. Separation of the $Au_{22}(dppee)_7$ Nanocluster by Chromatography

The $Au_{22}(dppee)_7$ product could be purified by column chromatography, as shown in Figure S1 (Supporting Information). The purified sample gave a single mass peak at m/z around 2478 as a triply charged cation in ESI-MS (Figure 1b) and the simulated isotopic distribution gave the precise formula of $[Au_{22}(dppee)_7H_3]^{3+}$. The UV-Vis-NIR spectrum of the freshly purified sample (Figure 2b) displayed distinct absorption peaks at 460, 380, and 310 nm, reflecting the molecular nature of the $Au_{22}(dppee)_7$ nanocluster. The distinct and well-resolved absorption spectrum also indicated the high purity of the column-separated sample. The stability of the $Au_{22}(dppee)_7$ nanocluster was tested in solution and the solid state. The UV-Vis-NIR spectra (Figure 2b) showed the new AuNC had a finite shelf life in the CH_2Cl_2 solution with significant changes observed after 3 d. After 6 d in solution, the absorption became significantly broadened and after 9 d the absorption curve was almost featureless. The purified $Au_{22}(dppee)_7$ nanocluster was relatively stable in the solid state under nitrogen atmosphere, but change was still observed after several days, as indicated by the UV-Vis-NIR spectrum shown in Figure 2b. Due to the stability problem, we were not able to successfully grow a single crystal of the $Au_{22}(dppee)_7$ nanocluster, despite of an extensive crystallization effort.

3. Discussion

The new $Au_{22}(dppee)_7$ nanocluster has the same gold core size as the previously reported $Au_{22}(dppo)_6$ cluster.[52] An important question was: do they have the same core structure? Since we were not able to obtain a single crystal for the new AuNC, we compared its properties with those of the $Au_{22}(dppo)_6$ cluster, in terms of UV-Vis-NIR and ^{31}P NMR. To obtain further structural information, we also carried out collision-induced dissociation (CID) experiments and compared the CID characteristics for both $[Au_{22}(dppee)_7H_3]^{3+}$ and $[Au_{22}(dppo)_6H_4]^{2+}$ using tandem ESI-MS. As will be shown below, we found that the Au_{22} cores were different in the two AuNCs with the slightly different ligands.

DOI: 10.1002/smll.201600407

3.1. UV-Vis-NIR Spectroscopy of Phosphine-Protected AuNCs

The UV-Vis-NIR spectra of phosphine-protected AuNCs are very distinguishable and characteristic of the core size and structures. The absorption bands between the 300 and 1000 nm UV-Vis-NIR spectral range are related to the electronic states of the gold core[62] and hence can be used to derive structural information. The absorption bands from the phosphine ligands are usually outside the 300–1000 nm spectral range. For gold cores with different nuclearity, or even the same nuclearity with different structures, the spectra will show totally different absorption peaks. For example, although both $[Au_6(dppp)_4]^{2+}$ and $[Au_7(dppp)_4]^{3+}$ have four 1,3-bis(diphenyl-phosphino)propane (dppp) ligands, their UV-Vis-NIR spectra show different peaks at 587 and 556 nm, respectively,[37] due to the different nuclearity. It has also been reported that the $[Au_6(dppp)_4]^{2+}$, $[Au_8(dppp)_4Cl_2]^{2+}$, and $[Au_{11}(dppp)_6]^{3+}$ clusters all have structures consisting of a gold core with addition atoms outside the core (core+exo) and they all have different absorption features, when compared with the core-only Au nanoclusters of the same nuclearity.[45,63] On the other hand, for the same gold core structure, or even different gold cores that share the same gold building units, the UV-Vis spectra always show similar absorption features, regardless of the phosphine ligands. For example, the $Au_{11}(PPh_3)_7Cl_3$ and $[Au_{11}(PPh_3)_8Cl_2]Cl$ clusters have the same Au_{11} core, but have different numbers of Cl and PPh_3 ligands.[46,64] Their UV-Vis-NIR spectra are very similar and show strong absorption peaks at ≈310 and 420 nm, and weak peaks at ≈380 and 515 nm, as documented in **Table 1**. Another example is the recently reported $[Au_{20}(PP_3)_4]Cl_4$ (PP_3 = tris[2-(diphenyl-phosphino)ethyl] phosphine, $C_{42}H_{42}P_4$) cluster,[50,51] which consists of an icosahedral Au_{13} building unit with an extra Au_7 clamp as a new layer. It was observed that the $[Au_{20}(PP_3)_4]Cl_4$ cluster gave similar UV-Vis-NIR spectral features as the previously known icosahedral cluster, $[Au_{13}(dppe)_5Cl_2]Cl_3$ (dppe = 1,2-bis(diphenyl-phosphino)ethane, $C_{26}H_{24}P_2$) at ≈360 and ≈490 nm.[65]

The UV-Vis-NIR spectrum of $Au_{22}(dppee)_7$ is compared with that of $Au_{22}(dppo)_6$ in **Figure 3** and they are not identical, suggesting the core geometry in the two AuNCs cannot be the same. However, the two spectra share a similar strong absorption band at ≈460 nm, as well as a band at ≈310 nm. Since the $Au_{22}(dppo)_6$ cluster consists of two fused Au_{11} units, the similar absorption features suggest the new $Au_{22}(dppee)_7$ nanocluster may also contain an Au_{11} unit. To test this hypothesis, we compared the UV-Vis-NIR spectra of the isolated Au_{11} nanocluster,[46,64] the previously reported $[Au_{20}(PPhPy_2)_{10}Cl_4]Cl_2$ nanocluster that contains two Au_{11} units sharing two Au atoms,[49] and the two Au_{22} nanoclusters in Table 1. The Au_{11} clusters protected by PPh_3 or PPh_3/Cl display strong absorption bands at ≈420 nm and ≈310 nm, in addition to weak absorptions at 515 nm and ≈380 nm. The two strong absorption bands are seen to be preserved in the $Au_{22}(dppo)_6$ and $[Au_{20}(PPhPy_2)_{10}Cl_4]Cl_2$ AuNCs, although slightly shifted because the latter two clusters contain fused Au_{11} units. These two absorption bands are also observed in the new $Au_{22}(dppee)_7$ cluster, suggesting it should also contain an Au_{11} unit. In addition, its strong absorption at 380 nm is also similar to that in the two Au_{11} clusters. The large shift of the 460 nm band in $Au_{22}(dppee)_7$ relative to the ≈420 nm band in the Au_{11} cluster suggests that the new Au_{22} cluster core is unlikely to be a polymer[66] or assembly[67] of isolated dppee-protected Au_{11} units. The CID and NMR data to be presented below are consistent with these observations.

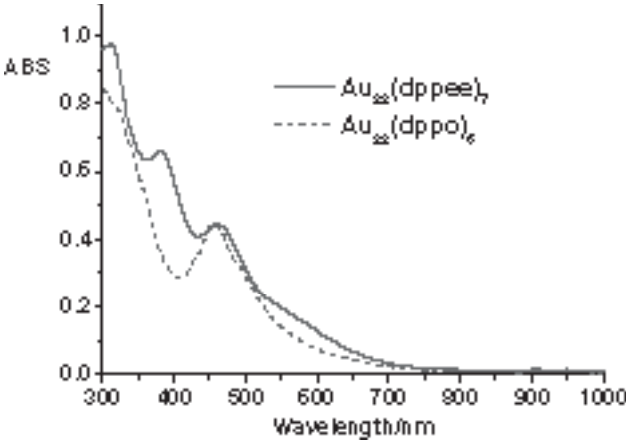

Figure 3. Comparison of the UV-Vis-NIR spectra of $Au_{22}(dppee)_7$ and $Au_{22}(dppo)_6$.

Table 1. Comparison of the main absorption bands in the UV-Vis-NIR spectra of Au22(dppee)$_7$, Au11(PPh3)$_7$Cl$_3$, [Au11(PPh3)$_8$Cl$_2$]Cl, Au22(dppo)$_6$, and [Au20(PPhPy2)$_{10}$Cl$_4$]Cl2. Strong peaks are in bold.

	Wavelength of the peaks [nm]				Reference
$Au22(dppee)_7$	–	**460**	**380**	310	Current work
$Au11(PPh3)_7Cl_3$	515	**420**	385	**308**	[46,64]
$[Au11(PPh3)_8Cl_2]Cl$	515	**416**	380	312	[46,64]
$Au22(dppo)_6$	–	**456**	–	313	[52]
$[Au20(PPhPy2)_{10}Cl_4]Cl2$	–	**493**	–	344	[49]

3.2. Collision-Induced Dissociations

To obtain further structural information, we carried out CID experiments of $Au_{22}(dppee)_7$ and compared them with those of $Au_{22}(dppo)_6$. In the positive-ion ESI-MS, many mass peaks were observed as protonated species because trace amount of formic acid was added to the mobile phase to facilitate the ESI (see the Experimental Section). Specifically, the $Au_{22}(dppo)_6$ cluster was observed previously in the form of $[Au_{22}(dppo)_6H_4]^{2+}$ (as well as alkali-complexed cations),[52] whereas the current $Au_{22}(dppee)_7$ cluster was observed in the form of $[Au_{22}(dppee)_6H_3]^{3+}$ (Figure 1). The proton was most likely associated with the P atom on the dppo ligands or the P and/or O atoms in the case of the dppee ligands. As shown in **Figure 4**, at low collision energies the CID of both Au_{22} nanoclusters showed very strong intensity (nearly 100%) for the parent molecular ions with relatively minor dissociations, indicating the thermal dynamic stability of both

small 2016,
DOI: 10.1002/smll.201600407

small NANO MICRO

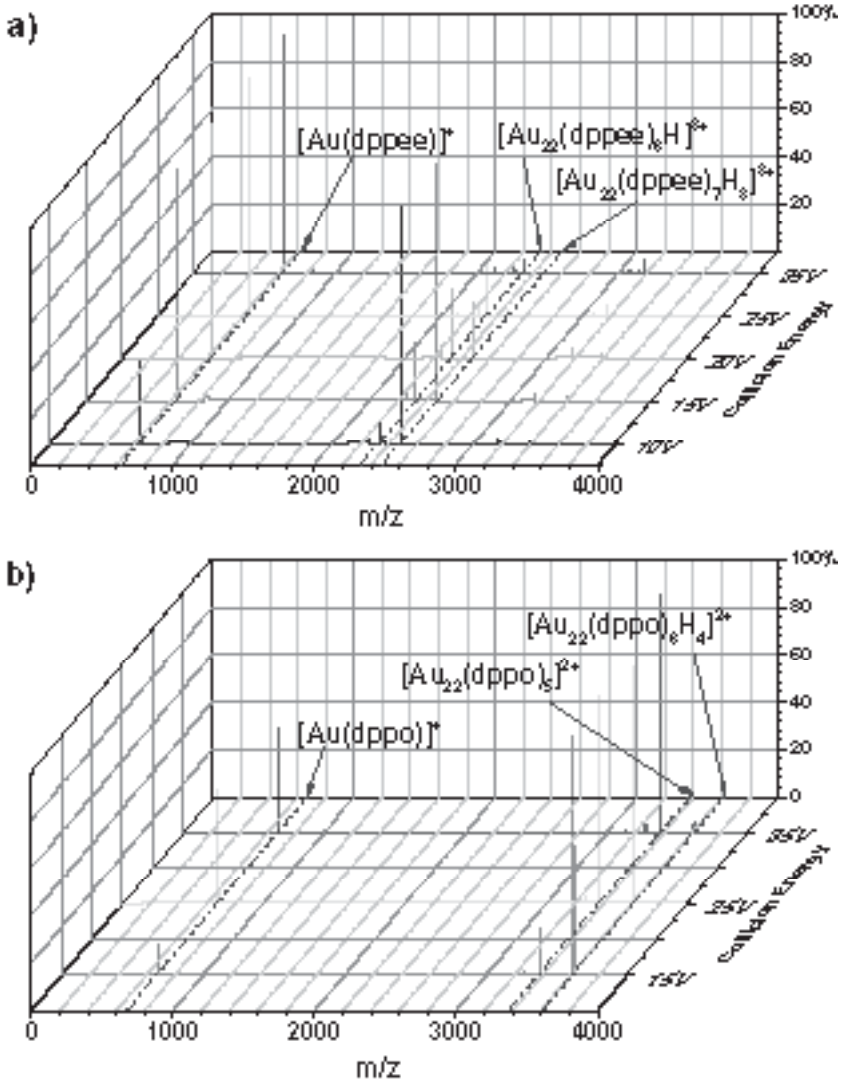

Figure 4. Collision-induced dissociation of a) $[Au_{22}(dppee)_7H_3]^{3+}$ and b) $[Au_{22}(dppo)_6H_4]^{2+}$ at different collision energies. (Mobile phase of ESI: acetonitrle/water = 50/50, 0.05% formic acid).

clusters. The major fragmentation channel in both cases was the loss of a gold atom and a ligand (L), i.e., AuL^+. It should be pointed out that the remaining heavier fragment after the loss of an AuL^+ unit would be beyond the mass range of our instrument and could not be detected in the tandem MS-MS mode. When the collision energy was increased, the mass spectra of both Au_{22} nanoclusters show weaker parent ion peaks, along with more fragmentation. The relative intensities of the different fragments as a function of collision energies are given in Figures S2 and S3 (Supporting Information) for $[Au_{22}(dppee)_6H_3]^{3+}$ and $[Au_{22}(dppo)_6H_4]^{2+}$, respectively. The $[Au_{22}(dppee)_6H_3]^{3+}$ parent ion was observed to be much less stable than the $[Au_{22}(dppo)_6H_4]^{2+}$ ion and was almost completely dissociated above the collision energy of 20 V (Figure S2, Supporting Information). In addition, many more fragments were observed for the $[Au_{22}(dppee)_6H_3]^{3+}$ parent ion than for the $[Au_{22}(dppo)_6H_4]^{2+}$ ion. Hence, in the gas-phase protonated forms, the CID experiments indicated that the $Au_{22}(dppee)_7$ cluster was more stable than $Au_{22}(dppo)_6$.

The major dissociation channels of $Au_{22}(dppee)_7$ involved the loss of dppee, Au(dppee), $Au(dppee)_2$, and $Au_2(dppee)_2$. At a given collision energy, the parent ion of $Au_{22}(dppo)_6$ displayed much less degree of dissociation (Figure 4b; Figure S3, Supporting Information). The different CID behaviors of the parent ions of $Au_{22}(dppee)_7$ and $Au_{22}(dppo)_6$ also suggested that they have different core structures. It should be pointed out that the CID of the phosphine ligand-protected Au_{11} cluster showed completely different behaviors from the two Au_{22} clusters.[68,69] The CID experiments are consistent with the UV-Vis-NIR data that the $Au_{22}(dppee)_7$ cluster may contain an Au_{11} unit, but with additional Au atoms coordinated around it. The ^{31}P-NMR data below provide similar structural hints for $Au_{22}(dppee)_7$.

3.3. ^{31}P-NMR

We have also used the ^{31}P NMR to characterize the new $Au_{22}(dppee)_7$ cluster. Although ^{31}P-NMR cannot give definitive structures, it is characteristic for different phosphine-protected AuNCs. For example, two icosahedral Au_{13} nanoclusters with different phosphine ligands[65,70] both show a single sharp ^{31}P peak at 66–67 ppm. The Au_{20} cluster with the Au_{13} building unit[50,51] also has a strong ^{31}P peak at 66–67 ppm. Another nanocluster with the Au_{13} building unit was Au_{19}, protected by N,N-bis(diphenylphosphino)amine and alkynylbenzene.[24] The single ^{31}P peak in Au_{19} was observed at 76 ppm; the shift was due to the stronger electron-withdrawing effect of the nitrogen atom. As for the nanoclusters with the Au_{11} building unit, such as $Au_{11}(PPh_3)_7Cl_3$, $[Au_{11}(PPh_3)_8Cl_2]Cl$, and $[Au_{20}(PPhPy_2)_{10}Cl_4]Cl_2$, they all have a single strong ^{31}P peak at 52–53 ppm.[46,49]

Figure 5 shows the ^{31}P-NMR spectrum of $Au_{22}(dppo)_6$ in comparison with that of $Au_{22}(dppee)_7$. In both spectra, numerous broad peaks were observed at 44–54 ppm, which were in the same range of chemical shifts of the phosphine ligands on the Au_{11} building unit. The multiplicity and broadening of the peaks could be explained by the relatively slow exchange rate between different ^{31}P nuclei. In principle, all the phosphorous atoms coordinated to the Au_{11} unit should have different chemical shifts, because of the asymmetric gold core. However, the fast exchange of small ligands like PPh_3 and $PPhPy_2$ makes these ^{31}P nuclei indistinguishable. Thus, only a single sharp peak was observed previously for $Au_{11}(PPh_3)_7Cl_3$, $[Au_{11}(PPh_3)_8Cl_2]Cl$, and

DOI: 10.1002/smll.201600407

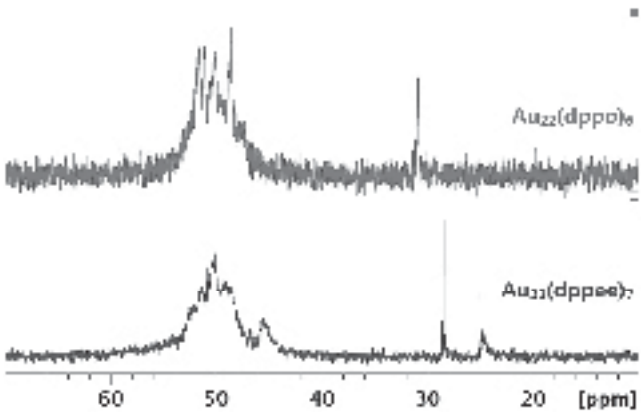

Figure 5. Comparison of the ^{31}P-NMR of $Au_{22}(dppo)_6$ and $Au_{22}(dppee)_7$ at 293 K.

$[Au_{20}(PPhPy_2)_{10}Cl_4]Cl_2$.[46,49] Since the migration of bulky long-chain ligands like dppee and dppo were much slower, multiple broad peaks were observed in $Au_{22}(dppo)_6$ and $Au_{22}(dppee)_7$. Additionally, the coupling between these chemically different ^{31}P nuclei could also contribute to the multiplicity and broadening. In order to further explore the existence of the dynamic behavior of the ^{31}P nuclei in $Au_{22}(dppee)_7$, we measured its ^{31}P-NMR at different temperatures, as shown in **Figure 6** (the chemical shifts of all peaks are given in Figures S4–S6, Supporting Information). At low temperatures, the exchange rate was slowed down, so that the ^{31}P-NMR peaks became sharper and better resolved. On the other hand, at high temperatures one expected the chemical shifts to coalesce, even though we did not try temperatures higher than 298 K due to concerns of decomposition.

In comparison, the ^{31}P-NMR of $Au_{22}(dppo)_6$ (Figure 5) also showed a single peak at ≈31 ppm, which was most likely due to the dppo oxide.[71] In the above CID study, we showed that the loss of a dppo ligand was the first dissociation channel for $Au_{22}(dppo)_6$ in the gas phase (Figure 4b). It was possible that in solution $Au_{22}(dppo)_6$ could also lose a ligand, which was then quickly oxidized to give the 31 ppm peak. In the ^{31}P-NMR of $Au_{22}(dppee)_7$, there were additional peaks at ≈28 and 25 ppm. We observed that the same 28 ppm peak also appeared in the ^{31}P-NMR of dppee as an impurity (Figure S7, Supporting Information). Since the only byproduct of dppee that gave similar chemical shifts after the column separation was dppee oxides, the 28 ppm peak in the ^{31}P-NMR of $Au_{22}(dppee)_7$ was also likely due to dppee oxides, similar to the ligand oxide in the $Au_{22}(dppo)_6$ cluster.

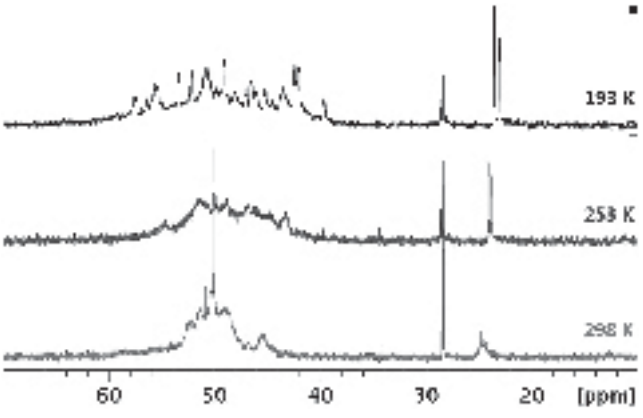

Figure 6. The ^{31}P-NMR of $Au_{22}(dppee)_7$ at 298, 253, and 193 K. Detailed chemical shifts are given in Figures S4–S6 (Supporting Information).

The peak at 25 ppm was a new feature that was not observed in the ^{31}P-NMR of $Au_{22}(dppo)_6$. It could be assigned to $Au_2Cl_2(dppee)$ by comparing with the ^{31}P-NMR of $Au_2Cl_2(dppee)$ (Figure S10, Supporting Information). However, unlike the sharp 28 ppm peak, the 25 ppm peak in ^{31}P-NMR of $Au_{22}(dppee)_7$ appeared as a doublet, which became sharper and more intense at low temperatures. The temperature effect of the 25 ppm doublet was similar to the peaks at 44–54 ppm, suggesting that it should belong to the $Au_{22}(dppee)_7$ nanocluster itself. These observations suggested that the $Au_{22}(dppee)_7$ cluster may contain motifs like $Au_2(dppee)$ at different positions. This conclusion is consistent with the structural inferences from both the UV-Vis-NIR and the CID results, that is, the $Au_{22}(dppee)_7$ cluster should contain an Au_{11} unit with additional coordination of $Au_2(dppee)$/$Au(dppee)$, which are likely in the exterior of the Au_{11} unit.

3.4. Summary of Structural Features of the $Au_{22}(dppee)_7$ Nanocluster

The UV-Vis-NIR, CID, and ^{31}P-NMR results are all consistent with the existence of an Au_{11} unit and additional $Au_2(dppee)$/$Au(dppee)$ in the $Au_{22}(dppee)_7$ nanocluster. However, unlike thiolate or alkynyl-AuNCs, there are unlikely Au-dppee staples in $Au_{22}(dppee)_7$. In the thiolate- or alkynyl-AuNCs, the ligands donate two pairs of electrons to Au,[72] one to the gold core and one to the Au atom in the staple. However, the P atom in phosphine ligands only has one pair of electrons available, and can only coordinate to one Au atom. Hence, the additional Au atoms in $Au_{22}(dppee)_7$ other than the Au_{11} unit should all form Au-Au bonds and are likely bonded to each other in some form, either as a new layer or as smaller clusters linked to the Au_{11} unit. On the basis of the stability of the $Au_{22}(dppee)_7$ cluster, we suspected that it might also contain uncoordinated Au atoms on the core surface, like those in $Au_{22}(dppo)_6$.

4. Conclusion

A new $Au_{22}(dppee)_7$ nanocluster has been synthesized with high purity and high yield. The dppee ligand is an analogue of the previous long-chain dppo ligand.[52] Characteristic UV-Vis-NIR absorption peaks at 460, 380, and 310 nm were observed for the $Au_{22}(dppee)_7$ cluster. Its precise molecular formula was determined by high-resolution electrospray mass spectrometry. The new AuNC was observed to have a shelf life of three to six days, making it difficult to grow single crystals. By comparing the UV-Vis-NIR, collision-induced dissociations, ^{31}P-NMR spectra of the new $Au_{22}(dppee)_7$, and the previous $Au_{22}(dppo)_6$ cluster, we concluded that $Au_{22}(dppee)_7$ has a different core structure, consisting of an

small 2016,
DOI: 10.1002/smll.201600407

Au_{11} unit with additional Au atoms most likely as a new layer on its surface. The current $Au_{22}(dppee)_7$ cluster and the previous $Au_{22}(dppo)_6$ cluster reveal that the Au_{22} nanoclusters exhibit interesting core isomers, depending on the ligands. Such structural polymorphism of phosphine-coordinated atom-precise gold clusters is intriguing and provides excellent systems for structure-property correlations.

5. Experimental Section

Chemicals: All chemicals were obtained from Sigma-Aldrich, and were used as received unless further noted. All solvents were technical grade unless further stated. All reactions under anhydrous conditions were conducted by using flame- or oven-dried glassware and standard syringe techniques under nitrogen atmosphere.

Characterizations: NMR spectra were recorded on both a 400 and a 600 MHz Bruker Ultrashield spectrometer using $CDCl_3$ or CD_2Cl_2 as solvent. Chemical shifts are reported in ppm and are referenced to tetramethylsilane (internal) for ^1H or ^{13}C-NMR and 85% H_3PO_4 (external) for ^{31}P-NMR. Unless further noted, all NMR spectra were measured at 298 K. UV–Vis-NIR spectra were measured in CH_2Cl_2 solution on a Varian Cary 50 Bio spectrophotometer. The mass spectra were measured in the positive ionization mode. The CH_2Cl_2 solution of AuNCs (≈0.5 mg mL^{-1}) was introduced into an Agilent 6530 Accurate Mass Q-TOF LC-MS system (with Agilent 1260 HPLC) via flow injection. The ESI mobile phase was made of acetonitrile/water (50/50) with ≈0.05% formic acid at a flow rate of 200 µL min^{-1}. The gas temperature of the ESI source was 130 °C at a flow rate of 8 L min^{-1}. The fragmentor voltage was set at 50 V, skimmer at 65 V, and the capillary voltage (V_{cap}) at 3500 V. The ESI-MS and collision-induced dissociation (CID) spectra were recorded at a rate of 1 spectrum s^{-1}. For the ESI-MS-CID experiment, the precursor parent ion was isolated with an m/z width of ≈4. The ESI-MS-CID spectra were acquired at collision energies of 15, 25, and 35 V. The mass range measured was up to 20 000 for MS and 4000 for MS/MS. The assignments were based on high-resolution m/z values and isotopic distributions.

Synthesis of the [bis(2-Diphenylphosphino)ethyl]Ether (dppee, $C_{28}H_{28}OP_2$) Ligand: 2-chloro-ethyl ether (2.5 mmol) was added to a 100 mL dry Schlenk flask. 20 mL tetrahydrofuran (THF) from a dry solvent dispensing system was then added to the Schlenk flask. After 15 min of vigorous stirring, potassium diphenylphosphide solution (10.5 mL, 0.5 M in dry THF) was slowly added to the system. The reaction was allowed to proceed for 24 h at 30 °C. After the removal of all solvents by a rotary evaporator, the product was extracted twice by 10 mL dichloromethane (DCM). The DCM extractions were combined and filtered. The filtrate was evaporated to give crude product. The pure product (≈75% yield) was obtained by silica gel column chromatography (hexanes/DCM), and characterized by NMR (Figures S7–S9, Supporting Information).

Synthesis of bis[chlorogold(I)][dppee] ($Au_2Cl_2(dppee)$, $C_{28}H_{28}OP_2Au_2Cl_2$): dppee (1 mmol) was added to a dry 50 mL Schlenk flask. DCM (5 mL) from a dry solvent dispensing system was added to the flask. After 20 min of vigorous stirring, chloro(dimethylsulfide)-gold(I) solution (20 mL, 0.1 mmol mL^{-1} in dry DCM) was quickly added to the system. The reaction was allowed to proceed for 36 h at 20 °C. After the removal of all solvents by a rotary evaporator, the product (≈95% yield based on Au atoms) was dried under vacuum for 12 h and stored under the protection of nitrogen. NMR was used to characterize the product (Figures S10–S14, Supporting Information).

Synthesis of $Au_{22}(dppee)_7$ Nanocluster: $Au_2Cl_2(dppee)$ (102 mg) was dissolved in 85 mL DCM. After vigorous stirring for 10 min at 20 °C, 3.5 mL ethanol solution of sodium borohydride (made by dissolving 41 mg sodium borohydride in 10 mL ethanol) was quickly added to the system. The reaction was allowed to proceed for 20 h before the removal of all solvents. Then the product was extracted twice by DCM (10 mL). The DCM extractions were combined, filtered and evaporated to dryness. The crude product was then purified by silica gel column chromatography (DCM/ethyl acetate/methanol = 8/2/3) to obtain a pure $Au_{22}(dppee)_7$ sample with a yield of ≈25% based on Au atoms.

Supporting Information

Supporting Information is available from the Wiley Online Library or from the author.

Acknowledgements

The authors would like to thank Dr. Tun-Li Shen for his help with the ESI-MS-CID experiments and Onkei Tai for her assistance with the low temperature NMR experiments.

[1] M. T. Pradeep, *Part. Part. Syst. Char.* **2014**, *31*, 1017.
[2] T. Tsukuda, H. Häkkinen, *Protected Metal Clusters: From Fundamentals to Applications*, Elsevier Science, Waltham, MA, USA, **2015**, 1–385.
[3] A. Das, C. Liu, H. Y. Byun, K. Nobusada, S. Zhao, N. Rosi, R. C. Jin, *Angew. Chem. Int. Ed.* **2015**, *54*, 3140.
[4] S. Chen, S. X. Wang, J. Zhong, Y. B. Song, J. Zhang, H. T. Sheng, Y. Pei, M. Z. Zhu, *Angew. Chem. Int. Ed.* **2015**, *54*, 3145.
[5] J. Zeng, C. Liu, Y. X. Chen, N. L. Rosi, R. C. Jin, *J. Am. Chem. Soc.* **2014**, *136*, 11922.
[6] A. Das, T. Li, K. Nobusada, C. J. Zeng, N. L. Rosi, R. C. Jin, *J. Am. Chem. Soc.* **2013**, *135*, 18264.
[7] A. Das, T. Li, G. Li, K. Nobusada, C. J. Zeng, N. L. Rosi, R. C. Jin, *Nanoscale* **2014**, *6*, 6458.
[8] D. Crasto, G. Barcaro, M. Stener, L. Sementa, A. Fortunelli, A. Dass, *J. Am. Chem. Soc.* **2014**, *136*, 14933.
[9] Y. B. Song, S. X. Wang, J. Zhang, X. Kang, S. Chen, P. Li, H. T. Sheng, M. Z. Zhu, *J. Am. Chem. Soc.* **2014**, *136*, 2963.
[10] M. W. Heaven, A. Dass, P. S. White, K. M. Holt, R. W. Murray, *J. Am. Chem. Soc.* **2008**, *130*, 3754.
[11] M. Zhu, C. M. Aikens, F. J. Hollander, G. C. Schatz, R. Jin, *J. Am. Chem. Soc.* **2008**, *130*, 5883.
[12] M. Z. Zhu, W. T. Eckenhoff, T. Pintauer, R. C. Jin, *J. Phys. Chem. C* **2008**, *112*, 14221.
[13] J. Zeng, T. Li, A. Das, N. L. Rosi, R. C. Jin, *J. Am. Chem. Soc.* **2013**, *135*, 10011.
[14] H. Y. Yang, Y. Wang, A. J. Edwards, J. Z. Yan, N. F. Zheng, *Chem. Commun.* **2014**, *50*, 14325.
[15] D. Crasto, S. Malola, G. Brosofsky, A. Dass, H. Hakkinen, *J. Am. Chem. Soc.* **2014**, *136*, 5000.

DOI: 10.1002/smll.201600407

[16] A. Das, C. Liu, C. J. Zeng, G. Li, T. Li, N. L. Rosi, R. C. Jin, *J. Phys. Chem. A* **2014**, *118*, 8264.
[17] S. Yang, J. S. Chai, Y. B. Song, X. Kang, H. T. Sheng, H. B. Chong, M. Z. Zhu, *J. Am. Chem. Soc.* **2015**, *137*, 10033.
[18] H. F. Qian, W. T. Eckenhoff, Y. Zhu, T. Pintauer, R. C. Jin, *J. Am. Chem. Soc.* **2010**, *132*, 8280.
[19] M. Azubel, J. Koivisto, S. Malola, D. Bushnell, G. L. Hura, A. L. Koh, H. Tsunoyama, T. Tsukuda, M. Pettersson, H. Hakkinen, R. D. Kornberg, *Science* **2014**, *345*, 909.
[20] P. D. Jadzinsky, G. Calero, C. J. Ackerson, D. A. Bushnell, R. D. Kornberg, *Science* **2007**, *318*, 430.
[21] Y. X. Chen, C. J. Zeng, C. Liu, K. Kirschbaum, C. Gayathri, R. R. Gil, N. L. Rosi, R. C. Jin, *J. Am. Chem. Soc.* **2015**, *137*, 10076.
[22] A. Dass, S. Theivendran, P. R. Nimmala, C. Kumara, V. R. Jupally, A. Fortunelli, L. Sementa, G. Barcaro, X. B. Zuo, B. C. Noll, *J. Am. Chem. Soc.* **2015**, *137*, 4610.
[23] A. Zeng, Y. Chen, K. Kirschbaum, K. Appavoo, M. Y. Sfeir, R. Jin, *Sci. Adv.* **2015**, *1*, e1500045.
[24] X. K. Wan, Q. Tang, S. F. Yuan, D. E. Jiang, Q. M. Wang, *J. Am. Chem. Soc.* **2015**, *137*, 652.
[25] X. K. Wan, S. F. Yuan, Q. Tang, D. E. Jiang, Q. M. Wang, *Angew. Chem. Int. Ed.* **2015**, *54*, 5977.
[26] X. K. Wan, W. W. Xu, S. F. Yuan, Y. Gao, X. C. Zeng, Q. M. Wang, *Angew. Chem. Int. Ed.* **2015**, *54*, 9683.
[27] K. Konishi, in *Gold Clusters, Colloids and Nanoparticles I*, Vol. *161* (Ed.: D. M. P. Mingos, Berlin, Germany), Springer International Publishing, **2014**, p. 49–86.
[28] A. Das, T. Li, K. Nobusada, Q. Zeng, N. L. Rosi, R. C. Jin, *J. Am. Chem. Soc.* **2012**, *134*, 20286.
[29] H. F. Qian, W. T. Eckenhoff, M. E. Bier, T. Pintauer, R. C. Jin, *Inorg. Chem.* **2011**, *50*, 10735.
[30] R. X. Jin, C. Liu, S. Zhao, A. Das, H. Z. Xing, C. Gayathri, Y. Xing, N. L. Rosi, R. R. Gil, R. C. Jin, *ACS Nano* **2015**, *9*, 8530.
[31] Y. B. Song, F. Y. Fu, J. Zhang, J. S. Chai, X. Kang, P. Li, S. L. Li, H. P. Zhou, M. Z. Zhu, *Angew. Chem. Int. Ed.* **2015**, *54*, 8430.
[32] Z. L. Wu, D. E. Jiang, A. K. P. Mann, D. R. Mullins, Z. A. Qiao, L. F. Allard, C. J. Zeng, R. C. Jin, S. H. Overbury, *J. Am. Chem. Soc.* **2014**, *136*, 6111.
[33] G. Li, H. Abroshan, Y. Chen, R. Jin, H. J. Kim, *J. Am. Chem. Soc.* **2015**, *137*, 14295.
[34] E. S. Smirnova, A. M. Echavarren, *Angew. Chem. Int. Ed.* **2013**, *52*, 9023.
[35] E. Briant, K. P. Hall, D. M. P. Mingos, A. C. Wheeler, *J. Chem. Soc., Dalton Trans.* **1986**, 687.
[36] J. W. A. van der Velden, J. J. Bour, J. J. Steggerda, P. T. Beurskens, M. Roseboom, J. H. Noordik, *Inorg. Chem.* **1982**, *21*, 4321.
[37] Y. Shichibu, M. Z. Zhang, Y. Kamei, K. Konishi, *J. Am. Chem. Soc.* **2014**, *136*, 12892.
[38] J. W. A. van der Velden, P. T. Beurskens, J. J. Bour, W. P. Bosman, J. H. Noordik, M. Kolenbrander, J. A. K. M. Buskes, *Inorg. Chem.* **1984**, *23*, 146.
[39] Y. Kamei, Y. Shichibu, K. Konishi, *Angew. Chem. Int. Ed.* **2011**, *50*, 7442.
[40] J. W. A. van der Velden, J. J. Bour, W. P. Bosman, J. H. Noordik, *J. Chem. Soc., Chem. Commun.* **1981**, 1218.
[41] K. P. Hall, B. R. C. Theoblad, D. I. Gilmour, D. M. P. Mingos, A. J. Welch, *J. Chem. Soc., Chem. Commun.* **1982**, 528.
[42] J. M. Smits, P. Beurskens, J. Bour, F. Vollenbroek, *J. Crystallogr. Spectrosc. Res.* **1983**, *13*, 365.
[43] J. Pethe, C. Maichle-Mössmer, J. Strähle, *Z. Anorg. Allg. Chem.* **1998**, *624*, 1207.
[44] M. T. Cheetham, M. M. Harding, J. L. Haggitt, D. M. P. Mingos, H. R. Powell, *J. Chem. Soc., Chem. Commun.* **1993**, 1000.
[45] Y. Shichibu, Y. Kamei, K. Konishi, *Chem. Commun.* **2012**, *48*, 7559.
[46] L. C. McKenzie, T. O. Zaikova, J. E. Hutchison, *J. Am. Chem. Soc.* **2014**, *136*, 13426.
[47] R. C. B. Copley, D. M. P. Mingos, *J. Chem. Soc., Dalton Trans.* **1996**, 479.
[48] S. Gutrath, I. M. Oppel, O. Presly, I. Beljakov, V. Meded, W. Wenzel, U. Simon, *Angew. Chem. Int. Ed.* **2013**, *52*, 3529.
[49] X. K. Wan, Z. W. Lin, Q. M. Wang, *J. Am. Chem. Soc.* **2012**, *134*, 14750.
[50] J. Chen, Q. F. Zhang, P. G. Williard, L. S. Wang, *Inorg. Chem.* **2014**, *53*, 3932.
[51] X. K. Wan, S. F. Yuan, Z. W. Lin, Q. M. Wang, *Angew. Chem. Int. Ed.* **2014**, *53*, 2923.
[52] J. Chen, Q. F. Zhang, T. A. Bonaccorso, P. G. Williard, L. S. Wang, *J. Am. Chem. Soc.* **2014**, *136*, 92.
[53] B. K. Teo, X. Shi, H. Zhang, *J. Am. Chem. Soc.* **1992**, *114*, 2743.
[54] G. Schmid, R. Pfeil, R. Boese, F. Bandermann, S. Meyer, G. Calis, J. W. A. van der Velden, *Chem. Ber.* **1981**, *114*, 3634.
[55] E. Gutiérrez, R. D. Powell, F. R. Furuya, J. F. Hainfeld, T. G. Schaaff, M. N. Shafigullin, P. W. Stephens, R. L. Whetten, *Eur. Phys. J. D* **1999**, *9*, 647.
[56] J. Li, X. Li, H.-J. Zhai, L.-S. Wang, *Science* **2003**, *299*, 864.
[57] Z. W. Wang, R. E. Palmer, *Nanoscale* **2012**, *4*, 4947.
[58] H.-F. Zhang, M. Stender, R. Zhang, C. Wang, J. Li, L.-S. Wang, *J. Phys. Chem. B* **2004**, *108*, 12259.
[59] M. F. Bertino, Z.-M. Sun, R. Zhang, L.-S. Wang, *J. Phys. Chem. B* **2006**, *110*, 21416.
[60] Z. T. Luo, V. Nachammai, B. Zhang, N. Yan, D. T. Leong, D. E. Jiang, J. P. Xie, *J. Am. Chem. Soc.* **2014**, *136*, 10577.
[61] M. Pettibone, J. W. Hudgens, *ACS Nano* **2011**, *5*, 2989.
[62] R. C. Jin, *Nanoscale* **2015**, *7*, 1549.
[63] Y. Shichibu, K. Konishi, *Inorg. Chem.* **2013**, *52*, 6570.
[64] X. Kang, Y. B. Song, H. J. Deng, J. Zhang, B. J. Liu, C. S. Pan, M. Z. Zhu, *RSC Adv.* **2015**, *5*, 66879.
[65] Y. Shichibu, K. Konishi, *Small* **2010**, *6*, 1216.
[66] M. De Nardi, S. Antonello, D. E. Jiang, F. F. Pan, K. Rissanen, M. Ruzzi, A. Venzo, A. Zoleo, F. Maran, *ACS Nano* **2014**, *8*, 8505.
[67] W. S. Compel, O. A. Wong, X. Chen, C. Yi, R. Geiss, H. Häkkinen, K. L. Knappenberger, C. J. Ackerson, *ACS Nano* **2015**, *9*, 11690.
[68] E. Bergeron, J. W. Hudgens, *J. Phys. Chem. C* **2007**, *111*, 8195.
[69] P. S. D. Robinson, T. L. Nguyen, H. Lioe, R. A. J. O'Hair, G. N. Khairallah, *Int. J. Mass Spectrom.* **2012**, *330*, 109.
[70] M. Sugiuchi, Y. Shichibu, T. Nakanishi, Y. Hasegawa, K. Konishi, *Chem. Commun.* **2015**, *51*, 13519.
[71] P. Calcagno, B. M. Kariuki, S. J. Kitchin, J. M. A. Robinson, D. Philp, K. D. M. Harris, *Chem. Eur. J.* **2000**, *6*, 2338.
[72] D. M. P. Mingos, *Dalton Trans.* **2015**, *44*, 6680.

Received: February 5, 2016
Revised: February 23, 2016
Published online:

DOI: 10.1002/smll.201600407